



HAL
open science

COMBINING MEASUREMENTS OR DATES USING HIERARCHICAL BAYESIAN STATISTICS: THE EVENT MODEL

Philippe Lanos, Anne Philippe

► **To cite this version:**

Philippe Lanos, Anne Philippe. COMBINING MEASUREMENTS OR DATES USING HIERARCHICAL BAYESIAN STATISTICS: THE EVENT MODEL. 2015. hal-01162404v1

HAL Id: hal-01162404

<https://hal.science/hal-01162404v1>

Preprint submitted on 10 Jun 2015 (v1), last revised 10 Dec 2015 (v3)

HAL is a multi-disciplinary open access archive for the deposit and dissemination of scientific research documents, whether they are published or not. The documents may come from teaching and research institutions in France or abroad, or from public or private research centers.

L'archive ouverte pluridisciplinaire **HAL**, est destinée au dépôt et à la diffusion de documents scientifiques de niveau recherche, publiés ou non, émanant des établissements d'enseignement et de recherche français ou étrangers, des laboratoires publics ou privés.

COMBINING MEASUREMENTS OR DATES USING HIERARCHICAL BAYESIAN STATISTICS: THE EVENT MODEL.

PHILIPPE LANOS¹ AND ANNE PHILIPPE²

Abstract

The most widely used methods for measurements or dates combination are the weighted mean and the *central age model* which are based on maximum likelihood (ML) estimation. However, these techniques do not take into account errors occurring between measurements or dates and the ML estimation does not operate when considering individual errors. This article proposes a new approach for combining measurements or dates through the *Event* model which is based on Bayesian statistics. This approach allows the estimation of a mean (mean of measurements or date of an Event from different datings) by introducing individual errors on each observation in addition to the experimental errors made during laboratory experiments. In particular, Event model implies that dates are coming from assumed contemporaneous artefacts. A prior information on these individual errors is introduced using the shrinkage density. This modelling provides a very simple way to automatically penalize outlying data with minimal assumptions about Bayesian parameters. The mathematical formulation is explained in details and many application examples are exhibited in different archaeological situations involving radiocarbon, luminescence and archaeomagnetic results. This new combination procedure is also applied to the wiggle-matching process in dendrochronological dating. Calculations are based on MCMC numerical techniques and can be performed using ChronoModel software which is freeware and multiplatform.

Keywords : Measurement combination, Event model, Bayesian statistics, individual errors, outlier penalization, MCMC methods, Chronomodel software

Date: June 9, 2015

¹ CNRS IRAMAT-CRPAA, Université Bordeaux-Montaigne and Géosciences-Rennes, Université Rennes 1.

² Laboratoire de mathématiques Jean Leray, Université Nantes.

This project is supported by the grant ANR-11-MONU-007 Chronomodel.

1. INTRODUCTION

The issue of combining measurements or dates currently occurs in physics and dating methods. The idea is to get a unique value with a confidence interval which summarizes a set of observations. The most widely used methods for measurements or dates combination are the weighted mean and the "central age model" which are based on maximum likelihood (ML) estimation. We make an overview of these techniques in this introduction. Thus, we consider the problem of combining measurements of the same unknown parameter when each measurement has its own uncertainty.

This question appears for determining a physical parameter from measurements which are done for example

- on a same object by several laboratories
- on different objects having the same physical parameter of interest.

In archeology this question arises for estimating the date of an event from a sample of n measurements done on contemporaneous artifacts by different dating methods. The measurement represents for instance:

- a ^{14}C age in radiocarbon,
- a paleodose measurement in luminescence (TL/OSL)
- an inclination, a declination or an intensity of the geomagnetic field in archaeomagnetism (AM)

They are converted into calendar dates using a calibration curve (see Section 3.1 for a description). This application plays an important role to constructing chronologies in archeology with software as BCal [Buck \(2004\)](#) or OxCal [Ramsey and Lee \(2013\)](#) [Bronk Ramsey \(2009a\)](#).

The statistical model is defined as n independent measurements M_1, \dots, M_n for which we assume that they have the same unknown mean μ . This is the parameter of interest. We denote s_i^2 the experimental variance on the measurement M_i , that are supposed known and evaluated by the laboratory during the measurement process. To summarize, we write

$$M_i = \mu + s_i \epsilon_i, \quad \forall i = 1, \dots, n \quad (1)$$

where $\epsilon_1, \dots, \epsilon_n$ are n independent identically distributed Gaussian random variables with zero mean and variance 1. The variances s_i^2 , $i = 1, \dots, n$. are supposed known and represent the measurement error.

As the measurements have different uncertainties, the empirical mean is not the right thing to calculate. Indeed, the estimator commonly used is the following weighted mean

(see [Ward and Wilson \(1978\)](#))

$$\hat{\mu}_n = \frac{\sum_{i=1}^n \frac{M_i}{s_i^2}}{\sum_{i=1}^n \frac{1}{s_i^2}} \quad (2)$$

Dating having high variances s_i^2 are thus penalized by the inverse of the variance when calculating the mean. Variance of estimator (2) is given by :

$$\text{var}(\hat{\mu}_n) = \frac{1}{\sum_{i=1}^n \frac{1}{s_i^2}}$$

The estimator $\hat{\mu}_n$ is the maximum likelihood estimate under the assumption that $\epsilon_1, \dots, \epsilon_n$ are Gaussian random variables. In this case $\hat{\mu}_n$ is an efficient estimate. (see [Appendix 5.1](#) for detail). This model is named "common age model" in [Galbraith et al. \(1999\)](#) for combining paleodose in luminescence dating method. This method is also implemented in Oxcal for combining 14C ages. (voir [Bronk Ramsey, 2009a](#)).

To take into account individual effect, we can add a random effect on the parameter μ . The model is then defined by

$$\begin{aligned} M_i &= \mu_i + s_i \epsilon_i \\ \mu_i &= \mu + \sigma \lambda_i \end{aligned} \quad (3)$$

where $\lambda_1, \dots, \lambda_n, \epsilon_1, \dots, \epsilon_n$ are $2n$ independent identically distributed Gaussian random variables with zero mean and variance 1. Error $\sigma \lambda_i$ represents the uncertainty between dating and the Event μ due to sampling (representativeness) problems of unknown origin which are not related to the measurement process itself in the laboratory. This model is named "central Age model" in [Galbraith et al. \(1999\)](#) and could be named here as "central measurement model". An explicit form of the likelihood estimate is not available. Consequently, numerical methods are required to approximate this estimate. See [Appendix 5.2](#) for details.

Alternatively, a Bayesian approach can be adopted to estimate the parameters μ and σ^2 of this hierarchical model. It is thus necessary to choose a prior distribution on (μ, σ^2) . This choice is discussed for instance in [Congdon \(2010\)](#) or [Spiegelhalter et al. \(2004\)](#) in the particular case of the meta-analysis. We decide not to discuss this approach of the Bayesian central model in this paper because the choice of the prior can be viewed as a particular case of our model studied in [Section 2](#) and [3](#). Indeed, we propose an extension of model (3) by including individual effects on the variance of λ_i . This approach is motivated

by the fact that each measurement can be affected by errors which can come from different sources (Christen (1994)) as:

- (1) the way to ensure that the samples studied can realistically provide results for the events that we wish to characterize (measurement or date)
- (2) the care in sampling in the field, the care in sample handling and preparation in the laboratory
- (3) other non-controllable random factors that can appear during the process.

Estimation of the mean using unknown individual variances σ_i^2 is achieved according to data nature: measurements alone or measurements calibrated into dates. For this model the ML estimate does not exist (See 5.3 for details). This is the reason why we propose a Bayesian approach described in Section 2 and Section 3.

The paper is organized as follows : Section 2 is devoted to Bayesian combinaison of measurements. We describe a hierarchical Bayesian model, which extend the age model. Two applications illustrate its performances. In section 3, we adapt our model for combining measurements to dating problems. We then define the so-called *Event model* to estimate a date from dating methods done on contemporary artefacts. In this case a calibration process is required to convert the measurements into dates. Our combinaison model is modified by adding a new stage in the hierarchical model.

Remark 1. *Throughout this article we define each Bayesian model using directed acyclic graph (DAG). This graph describes the dependencies in the joint distribution of the probabilistic model. Each random variable of the model (that is an observation or a parameter) appears as a node in the graph. Any node is conditionally independent of its non-descendents given its parents. Hereafter the circle correspond to all the random variables of the model. With the color of the circles, we distinguish between observations (red) and parameters (blue).*

2. COMBINING MEASUREMENTS USING BAYESIAN APPROACH

2.1. The Model. We want to estimate a parameter μ from n measurements (M_1, \dots, M_n) , which are modelled by random variables with mean value μ .

We propose in this section an extension of the central age model defined in (3), which includes individual effects on the variance. We describe now our hierarchical Bayesian model. At the first stage we introduce latent variables μ_i to take into account unknown individual errors affecting the measurements :

$$M_i = \mu_i + s_i \epsilon_i$$

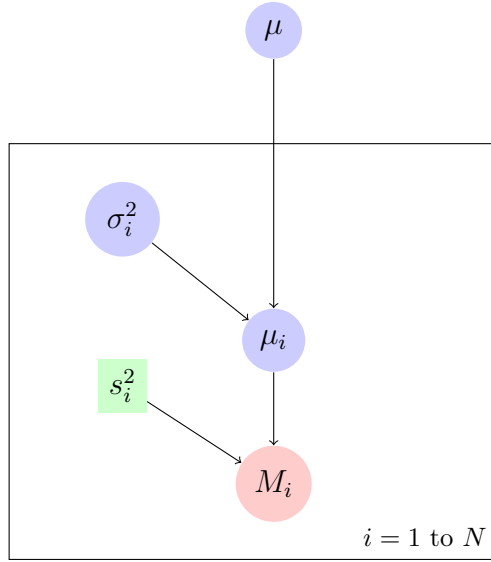


FIGURE 1. DAG of the Bayesian model for combining measurements.

where $\epsilon_1, \dots, \epsilon_n$ are n independent identically distributed Gaussian random variables with zero mean and variance 1.

On the latent variables μ_i , $i = 1, \dots, n$ we assume that

$$\mu_i = \mu + \sigma_i \lambda_i \quad (4)$$

where $\lambda_1, \dots, \lambda_n$ are n independent identically distributed Gaussian random variables with zero mean and variance 1. The individual effects occur through the individual variances σ_i^2 which are supposed unknown. Their prior distributions is defined in Section 2.2.

The hierarchical Bayesian model for combining measurements is summarized by the DAG in Figure 1. According to this diagram the joint density is of the form

$$p(M_1, \dots, M_n, \mu_1, \dots, \mu_n, \sigma_1^2, \dots, \sigma_n^2, \mu) = \prod_{i=1}^n p(M_i | \mu_i) \prod_{i=1}^n p(\mu_i | \sigma_i^2, \mu) \prod_{i=1}^n p(\sigma_i^2) p(\mu) \quad (5)$$

where, for all $i = 1, \dots, n$ ¹

$$\begin{aligned} M_i | \mu_i &\sim \mathcal{N}(\mu_i, s_i^2) \\ \mu_i | \mu, \sigma_i^2 &\sim \mathcal{N}(\mu, \sigma_i^2). \end{aligned}$$

We discuss now the choice of the prior distributions on the parameter of interest μ and the individual variances σ_i^2 .

¹The notation $X|Y$ is used for the conditional distribution of X given Y .

2.2. Choice of the prior on σ_i^2 and μ . The parameter of interest μ is assumed to be uniformly distributed on an interval $T = [t_m, t_M]$. The length of this interval depends on the prior information available.

For the hyperparameters σ_i^2 in the third stage of the hierarchical model, the choice of a diffuse noninformative prior may be problematic as improper priors may induce improper posteriors.

This problem appears, for example, if we apply the Jeffreys prior (obtained for Gaussian observations) $1/\sigma_i^2$ to variances of our model with individual random effects. The choice of diffuse priors in such models raises particular issues, discussed for instance in [Congdon \(2010\)](#) (see page 33 and 90).

It is always possible to choose a proper probability distribution which approximates the diffuse prior as for instance

- a density proportional to the Jeffreys prior truncated on a compact set in $]0, \infty[$,
- an inverse Gamma distribution with small scale and shape parameters.

However, such priors may cause identifiability problems as the posteriors are close to being empirically improper. Moreover the inference about the parameter of interest is very sensitive to choice of parameters of the proper prior distribution.

Among many alternatives proposed in the literature, we choose the uniform shrinkage distribution introduced by [Daniels \(1999\)](#). This probability distribution admits a density, given by

$$p(\sigma_i^2) = \frac{s_0^2}{(s_0^2 + \sigma_i^2)^2}. \quad (6)$$

where the parameter s_0^2 must be fixed. Note that this form of density implies that the random variable $s_0^2/(\sigma^2 + s_0^2)$ is uniformly distributed on $[0, 1]$. The variance and mean of this distribution are infinite, so it can be considered as weakly informative.

In the particular case of the central age model, [Spiegelhalter et al. \(2004\)](#) suggests the following choice of parameter :

$$\frac{1}{s_0^2} = \frac{1}{n} \sum_{i=1}^n \frac{1}{s_i^2}$$

Hereafter we take this choice of parameter for the different numerical examples.

Remark 2. *It is possible to extend the uniform shrinkage by taking*

$$p(\sigma_i^2) = \frac{as_0^{2a}}{(s_0^2 + \sigma_i^2)^{a+1}}.$$

In this case $\sigma_i^2 = u - s_0^2$ where u is distributed according to the Pareto distribution with parameters (a, s_0) , that is $P(\sigma^2 > t) = (t/s_0^2)^{-a}$ for all $t > s_0^2$. When a tends to zero, we obtain the Jeffreys prior.

2.3. MCMC algorithm. The posterior distribution of the parameter of interest μ can not be obtained explicitly. It is required to implement an MCMC algorithm to approximate the posterior distribution, its quantiles, the Bayes estimates and the HPD regions.

As all the full conditionals cannot be simulated by standard random generators, we adopt the Metropolis-within-Gibbs strategy. For each parameter, the full conditional distribution is proportional to (5).

- (1) For the parameter of interest μ and the latent variables μ_i , we identify a truncated Gaussian distribution on the study period T . Such a distribution can be simulated using rejection sampling. Different choices of proposal are possible as the Gaussian distribution or the truncated Laplace (double exponential) distribution on T . It is also possible to use an adaptive random walk MH with a Gaussian proposal.
- (2) The density of the full conditional distribution of σ_i^2 is explicitly computable up to an unknown multiplicative constant, but it is not a standard distribution. Therefore it is simulated using an adaptive random walk MH with a Gaussian proposal on the variable $\log(\sigma_i^2)$.

These algorithms are implemented in Chronomodel software, which is freeware and multiplatform. It can be downloaded on the following website <http://www.chromodel.fr>. See [Chronomodel Software \(2015\)](#); [Vibet et al. \(2015\)](#) for details. In the applications discussed below, the graphics summarizing the numerical results are performed using ChronoModel software. We represent the marginal densities of

- the parameter of interest μ (on gray background)
- the individual measurements μ_i (on white background)
- the individual standard deviations σ_i

For each density, the bar above the density represents the shorter 95% posterior probability interval. The vertical lines, delimiting the colored area under the density curve, indicate the endpoints of the 95% highest posterior density (HPD) region. For unimodal posterior density, both 95% posterior probability regions coincide.

2.4. Application to sample of measurements.

Example 1. Mean paleodose calculation in OSL dating

As a first illustration, Figures 2-3 show an example (denoted Yem-11) of a mean paleodose calculated from 18 individual aliquots for sample SD1-08OSL11 of Shi Bat Dihya 1,

in Wadi Surdud middle paleolithic site complex (Yemen) (see [Sitzia et al. \(2012\)](#)). Determinations are based on Analyst software and measurement unit is in Gy/ka. Results here are presented in Age obtained by dividing the equivalent aliquot paleodoses by the dose rate (see table II, p. 477 [Sitzia et al., 2012](#)).

Application of the finite Mixture Model ([Galbraith and Green \(1990\)](#)) leads to an equivalent dose of 56 ± 5 , that is $[46, 66]$ at 95%. Alternatively, the ML estimate given by (2) is equal to $\hat{\mu}_n = 42.8$ and the frequentist confidence interval is $[40.6, 45.1]$. This approach seems to provide accurate estimation however, there is a lack of robustness. Indeed, if we delete the observation `yem-11_9`, the ML estimate is 57.05 and the confidence interval is $[54.7, 59.4]$ at 95%. So, the results are very sensitive to this value, which seems to be an outlier. However, looking at Figure 2, it is difficult to decide which aliquots can be deleted for the estimation.

The Bayesian model doesn't need to select data or penalize some of them. Taking all the aliquots, it provides the HPD interval $[50, 59]$ at 95% confidence level, which is much more precise than the one obtained with the finite mixture.

Example 2. Mean intensity calculation in archaeomagnetic dating

The second example in Figure 4 and 5 deals with the mean of a set of intensities in archaeomagnetic dating. Archaeo-intensities have been determined from 17 different bricks coming from Notre-Dame-sous-Terre (NDST) church in Mont-Saint-Michel abbey (Normandy, France), building state 1 ([Sapin et al., 2008](#), see table D page 107). The ML estimate given by (2) is equal to $\hat{\mu}_n = 68.5$ and the frequentist confidence interval is $[68, 69.2]$. The Event model provides the HPD interval $[68, 71]$ for the parameter μ at 95% confidence level. In this case, the Bayesian approach leads to a wider HPD interval than the frequentist one because it takes into account the scattering of the dates.

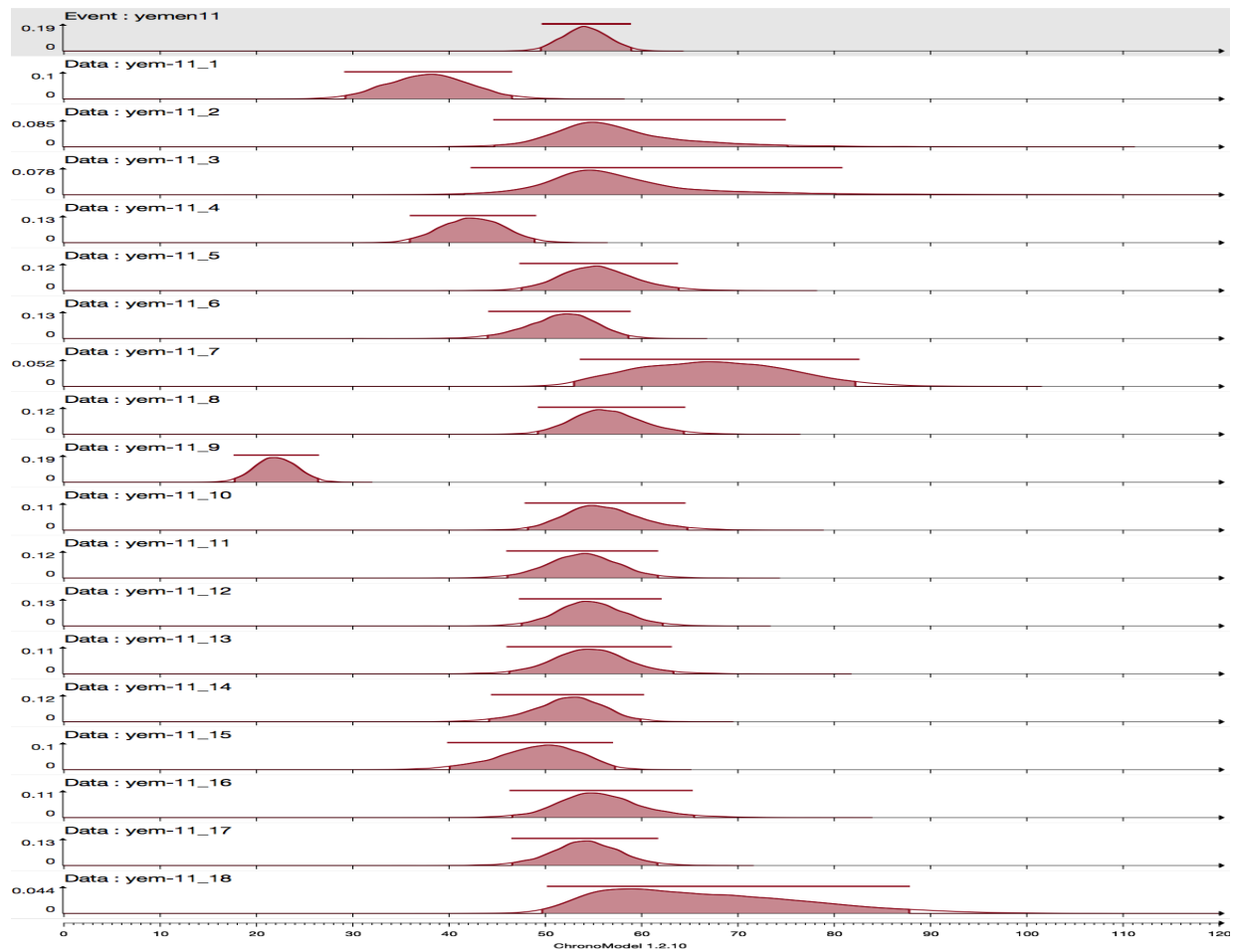


FIGURE 2. Yemen, Ex. 1. Posterior densities of μ_i , $i = 1, \dots, 18$ (white background) and μ (gray background) for the Paleodose estimation on the sample Yem-11.

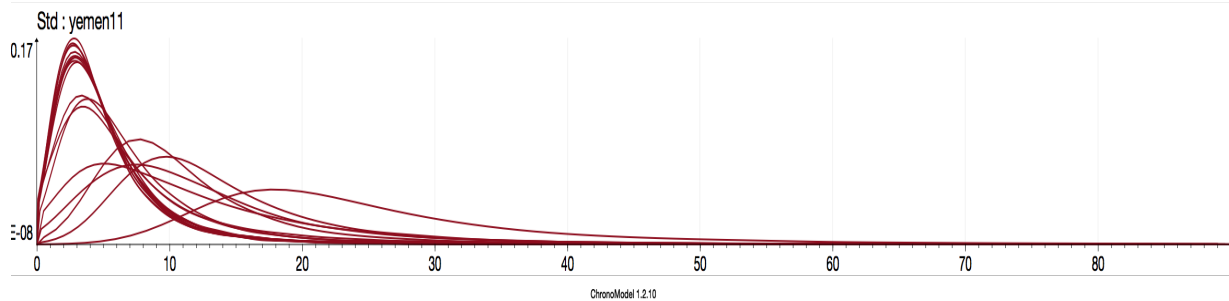


FIGURE 3. Yemen, Ex. 1 (cont.). Posterior densities obtained for the standard deviations σ_i , $i = 1, \dots, n$.

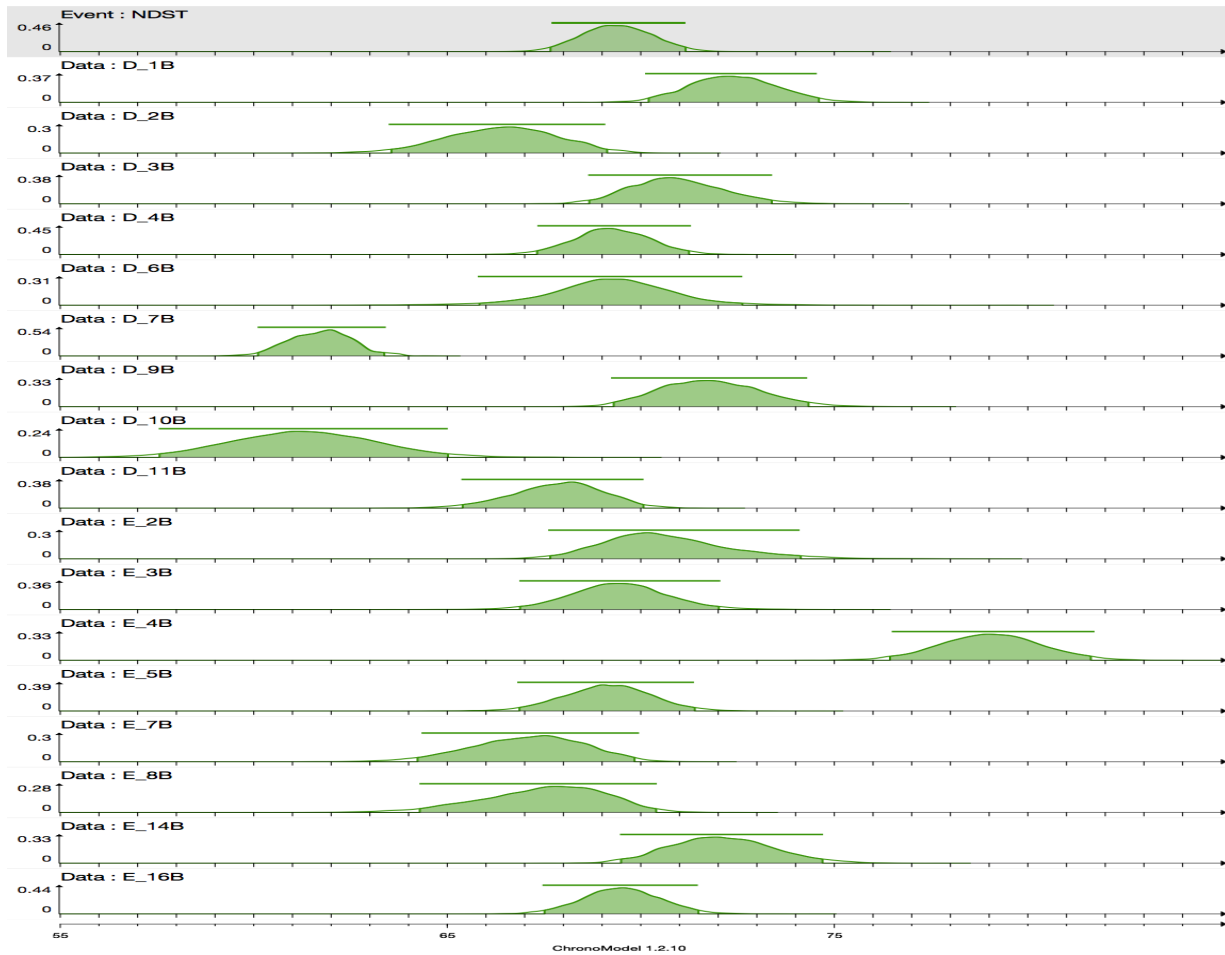


FIGURE 4. NDST, Ex 2. Posterior densities of μ_i , $i = 1, \dots, 18$ (white background) and μ (gray background) for the archeo-intensity

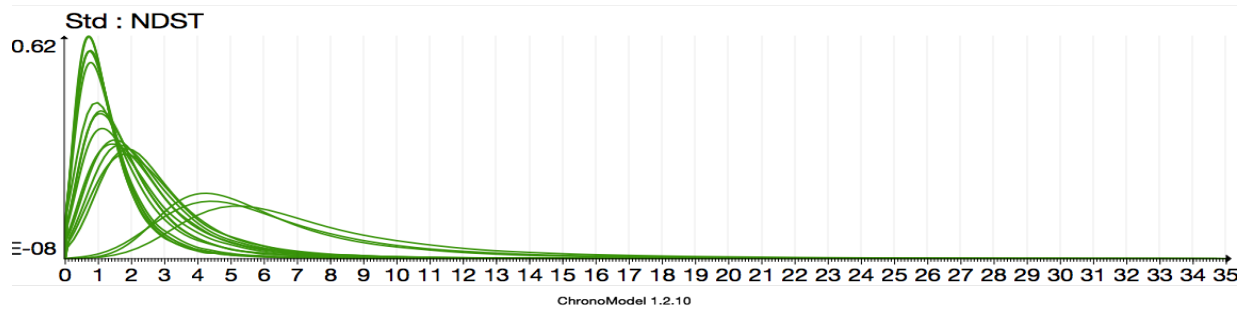


FIGURE 5. NDST, Ex 2 (cont.). Posterior densities obtained for the standard deviations σ_i , $i = 1, \dots, n$.

3. EVENT MODEL FOR DATING COMBINATION WITH CALIBRATION

At the beginning of this section, we recall some Bayesian models implemented in Oxcal, that are the individual calibration and the combination of 14C dates.

3.1. Individual calibration. The simplest problem is the calibration of a measurement M in calendar time t . The measure M has a Gaussian distribution with mean μ and unknown variance s^2 . This is a hierarchical model, the variable μ has also a Gaussian distribution with mean $g(t)$ and variance $\sigma_g^2(t)$ where g is a function called "calibration curve" linking the measurement to calendar time t . Every dating method has its own calibration curve. For instance, the curve IntCal09 converts a radiocarbon Age in calendar date for the mainland samples. This is the dendrochronological calibration of 14C ages. [Ramsey and Lee \(2013\)](#); [Manning and Kromer \(2011\)](#); [Bronk Ramsey \(2009a\)](#); [Buck \(2004\)](#); [Buck et al. \(1996\)](#); [Litton and Buck \(1995\)](#).

In archaeomagnetism the secular variation curves of the Earth's magnetic field are used to convert a inclination, declination or intensity measurement to calendar date. In the case of an age M provided by Luminescence (TL or OSL), the calibration function is just a linear function $g(t) = (t - t_0)$ where t_0 is the determination year of the age measurement M in the laboratory.

The Bayesian model for 'calibration' or conversion of a measure M to calendar date t is described below. The model on the measurement M is given by

$$M = \mu + s\epsilon$$

where μ is the true value of the measurement, and where s^2 is the known variance. The distribution of ϵ is the standard Gaussian distribution.

The calibration step converts μ to a calendar date t , using the relation

$$\mu = g(t) + \sigma_g(t)\rho$$

where both functions g and σ_g are supposed known, and where ρ is a standard Gaussian random variable.

Let T be the range of study. We choose the uniform distribution on T as prior distribution on the parameter t ,

$$p(t) \propto 1_T(t) \tag{7}$$

If we integrate the posterior distribution of (t, μ) with respect to latent variable μ , we get the posterior distribution of t (up to a multiplicative constant) :

$$p(t|M) \propto \frac{1}{S(t)} \exp\left(\frac{-1}{2S^2(t)}(M - g(t))^2\right) 1_T(t) \tag{8}$$

where

$$S(t)^2 = s^2 + \sigma_g^2(t) \quad (9)$$

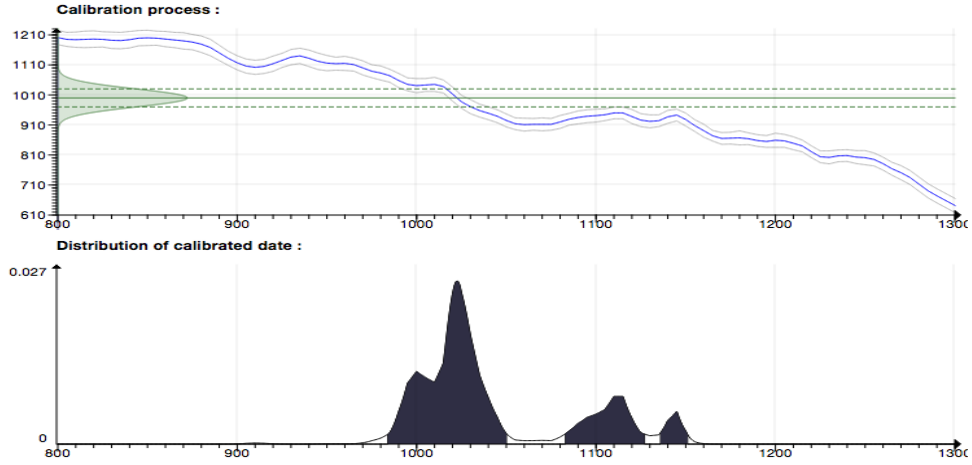


FIGURE 6. Conversion of a ^{14}C age ($A = 1000 \pm 30$ BP) in calendar date via the calibration curve IntCal13

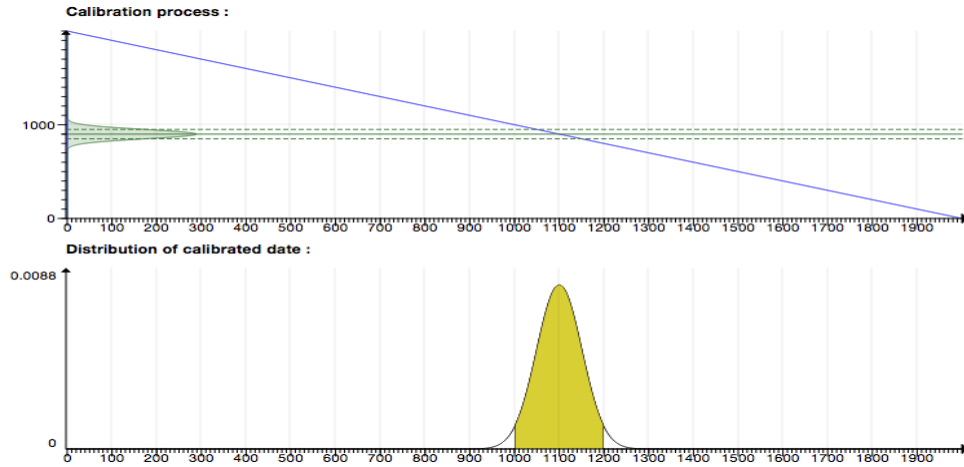


FIGURE 7. Conversion of a TL age ($A = 900 \pm 50$) in calendar date through the linear transformation $g(t) = (2000 - t)$

3.2. Calibration from multiple measurements (R-Combine in Oxcal). We observe m independent measurements M_k performed on a same object. This appears for example in the case of radiocarbon dating when the same object is analyzed by different laboratories.

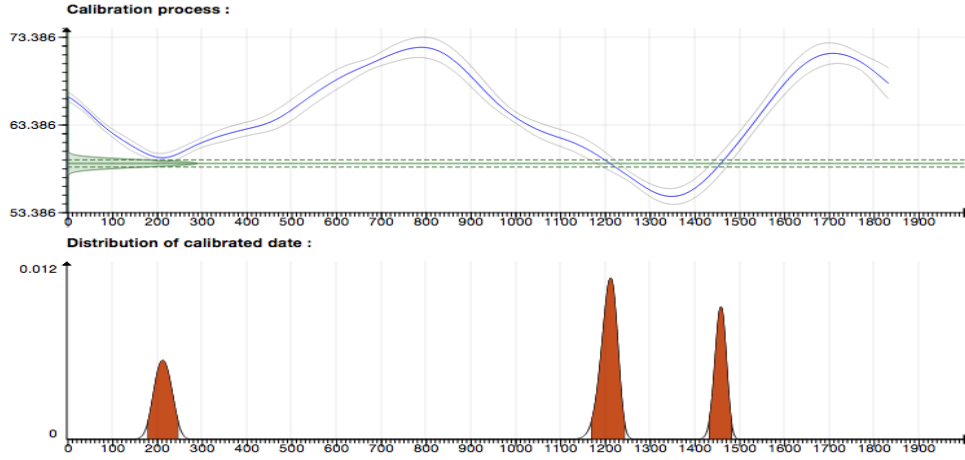


FIGURE 8. Conversion of an inclination measurement ($I = 59 \pm 1$) in calendar date via the calibration curve of archaeomagnetic field in France (Paris) during the last two millennia.

In this case, measurements have to be combined before calibration (see [Ward and Wilson \(1978\)](#) and [Bronk Ramsey \(2009a\)](#)). This approach requires that all the measurements have the same calibration curve.

According to the DAG given in Figure 9, the Bayesian model is defined by the following distributions :

$$\begin{aligned} M_i | \mu &\sim \mathcal{N}(\mu, s_i^2) \quad \forall i = 1, \dots, n \\ \mu | t &\sim \mathcal{N}(g(t), \sigma_{g(t)}^2) \\ t &\sim \text{Unif}(T). \end{aligned}$$

One can easily get the marginales posterior density of t , which is given by

$$p(t | M_1, \dots, M_m) \propto \frac{1}{\tilde{S}_m(t)} \exp\left(\frac{-1}{2\tilde{S}_m(t)^2} (\bar{M} - g(t))^2\right) 1_T(t)$$

where

$$\tilde{S}_m(t)^2 = \bar{s}^2 + \sigma_g^2(t) \quad \text{with} \quad \frac{1}{\bar{s}^2} = \sum_{k=1}^m \frac{1}{s_k^2}$$

and where

$$\bar{M} = \sum_{k=1}^m \frac{M_k}{s_k^2} / \sum_{k=1}^m \frac{1}{s_k^2}.$$

The R-combine model is equivalent to the individual calibration of the observation (\bar{M}, \bar{s}^2) using the process described in Section 3.1.

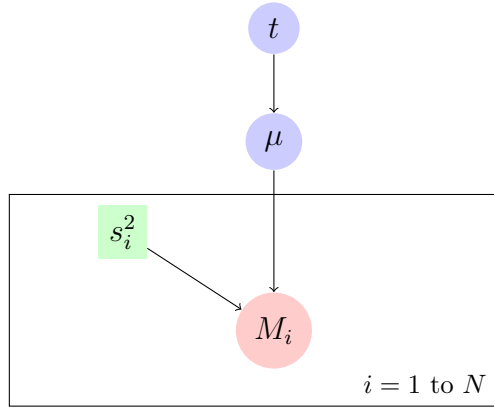


FIGURE 9. DAG of the R-Combine model.

3.3. Calibrated Event. In the general case we observe n measurements M_i such that each measurement provides a dating through a calibration step defined by a calibration function g_i and its error σ_{g_i} . The R-combine model is not longer valid in this case since it requires a common calibration curve (i.e. $g_i = g$ for all $i = 1, \dots, n$). Our idea is to adapt the Bayesian combinaison of measurements to estimate the date of an archaeological event from individual datings of contemporaneous artefacts.

3.3.1. The model. We describe the so-called Event model to estimate a date θ from n measurements M_i provided by different dating methods. We assume that each measurement M_i is related to an individual date t_i through a calibration curve g_i . Here this curve is supposed known with some known uncertainty. The main assumption in our Event model is the contemporaneity of the dates t_i , $i = 1, \dots, n$ with the event date θ .

In this context the model with random effect given by (3) can be rewritten as follows

$$\begin{aligned}
 M_i &= \mu_i + s_i \epsilon_i \\
 \mu_i &= g_i(t_i) + \sigma_{g_i(t)} \rho_i \\
 t_i &= \theta + \sigma_i \lambda_i
 \end{aligned} \tag{10}$$

where $(\epsilon_1, \dots, \epsilon_n, \rho_1, \dots, \rho_n, \lambda_1, \dots, \lambda_n)$ are independent identically distributed Gaussian random variables with zero mean and variance 1.

The random variables $(\lambda_i)_i$ and $(\epsilon_i)_i$ are independent and satisfy the following properties :

- $\sigma_i \lambda_i$ represents the error between t_i and θ due to sampling problems external to the laboratory (see Section 1).
- $s_i \epsilon_i + \sigma_{g_i(t)} \rho_i$ represents the experimental error provided by the laboratory and the calibration error

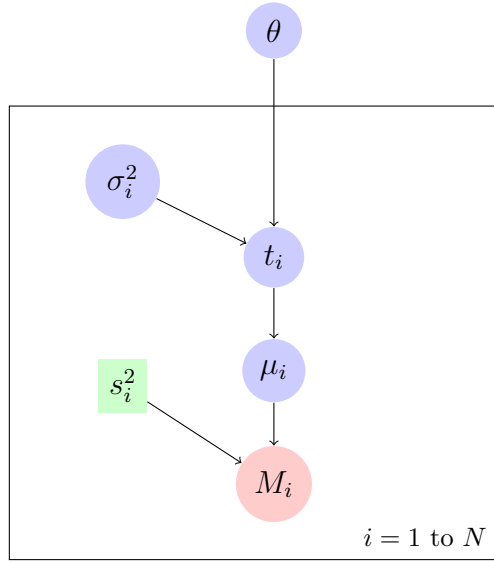


FIGURE 10. DAG for the hierarchical Event model applied to dating combination with calibration.

According to the DAG defining the event model (see Figure 10) the joint distribution of the probabilistic model can be write of the form

$$p(M_1, \dots, M_n, \mu_1, \dots, \mu_n, t_1, \dots, t_n, \sigma_1^2, \dots, \sigma_n^2, \theta) = p(\theta) \prod_{i=1}^n p(M_i|\mu_i)p(\mu_i|t_i)p(t_i|\sigma_i^2, \theta)p(\sigma_i^2), \quad (11)$$

where the conditional distributions, that appear in the decomposition are given by

$$\begin{aligned} M_i|\mu_i &\sim \mathcal{N}(\mu_i, s_i^2) \\ \mu_i|t_i &\sim \mathcal{N}(g_i(t_i), \sigma_{g_i}(t_i)^2) \\ t_i|\sigma_i^2, \theta &\sim \mathcal{N}(\theta, \sigma_i^2) \end{aligned} \quad (12)$$

$$\sigma_i^2 \sim \text{Shrink}(s_0^2) \quad (13)$$

$$\theta \sim \text{Unif}(T) \quad (14)$$

The density of the shrinkage distribution with parameter s_0^2 , that appears in (13), is given by (6).

With calibrated measurements, the parameter s_0^2 cannot be calculated directly from the variances s_i^2 as explained in Section 2.2. Indeed the measurement errors s_i are not necessarily homogeneous units (see for instance the case of archaeomagnetism combined with 14C).

We proceed in the following way, for each $i = 1, \dots, n$:

- (1) an individual calibration step is done for each measurements M_i
 - (a) we compute the posterior distribution of t_i (using (8))
 - (b) we approximate the posterior variance $\widehat{s}_i^2 = \text{var}(t_i|M_i)$
- (2) We take as shrinkage parameter s_0 :

$$\frac{1}{s_0^2} = \frac{1}{n} \sum_{i=1}^n \frac{1}{\widehat{s}_i^2}$$

3.3.2. *Typo-chronological information or Reference chronological information.* This is the case of dating provided by the study of objects recovered during excavations. The datings are often expressed in the form of time intervals $[t_{im}, t_{iM}]$. Thus, the observations are both dates (t_{im}, t_{iM}) . They correspond to an interval which contains the unknown date t_i which does not come from measurement.

In this special case a possible choice of model is the following : we assume that conditionnaly to t_i , the random variables (t_{im}, t_{iM}) are independent

$$p(t_{im}, t_{iM}|t_i) = p(t_{im}|t_i)p(t_{iM}|t_i)$$

and they are distributed from truncated exponential distribution with parameter $\lambda > 0$. The supports are respectively $] -\infty, t_i]$ and $[t_i, +\infty[$. The resulting density is of the form

$$p(t_{im}, t_{iM}|t_i) = \lambda^2 e^{-\lambda(t_{im}-t_{iM})} 1_{t_{im} \leq t_i \leq t_{iM}}$$

Remark 3. *The parameter λ does not appear in the posterior distribution. So it can be fixed arbitrarily equal to 1.*

For the other parameters of the event model, we keep the same distribution as defind in (12),(13) and (14).

3.4. **MCMC algorithm.** We keep the same algorithm as that described in Section 2.3 except for the latent variables t_i . The full distribution of t_i , $i = 1, \dots, n$, is proportional to

$$\frac{1}{S_i(t_i)} \exp \left\{ \frac{-1}{2S_i^2(t_i)} (M_i - g_i(t_i))^2 \right\} \exp \left\{ \frac{-1}{2\sigma_i^2} (t_i - \theta)^2 \right\} 1_T(t_i)$$

where $S_i(t_i)$ is defined in (9). We can choose an adaptive random walk MH with a Gaussian proposal. But the random walk solution is not necessarily the most efficient choice because the target distribution can be multimodal. We are frequently confronted to this problem with the dating results. See for instance the results given by Archaeomagnetic dating in Ex. 5 and Ex. 6 In this context, an alternative is to choose an independent Metropolis-Hastings algorithm with the individual calibration density as proposal. This ensures that all the possible values of t_i can be visited when the calibrated date distribution is multimodal.

3.5. Applications.

Example 3. Shroud of Turin (Italy)

As a first example of Event model applied to dating combination with calibration, we consider the shroud of Turin dated by radiocarbon (see [Damon \(1989\)](#)). Twelve radiocarbon datings have been performed on a strip cut from the shroud and divided into three samples sent to Arizona, Oxford and Zurich AMS laboratories. Four, three and five determinations were made respectively. Christen (see page 498-499 [Christen, 1994](#)) calculated a combination (R-combine procedure) with outlier detection. Removing determinations A1.1 and O1.1, the HPD interval obtained by Christen is [1267, 1313] AD at 95%. In this case, the Event model (Fig. 11) taking into account all the dates without rejection, gives a very close HPD interval equal to [1265 ; 1315] at 95%.

Example 4. Mont-Saint-Michel (Normandy, France), Notre-Dame-sous-Terre Church.

Here we take dates of building state 1 from the carolingian church Notre-Dame-sous-Terre (NDST) in Mont-Saint-Michel (Normandy, France) (see pages 110-116 [Sapin et al., 2008](#)). Dating is based on 3 charcoals (^{14}C dating) and 8 bricks (TL dating) (Fig. 13). Event model gives a HPD interval equal to [898 ; 987] at 95% probability level. Posterior densities for standard deviations σ_i^2 remain concentrated onto small ranges [0, 200] at 95% (Fig. 14), which are of the same order as errors on individual dates themselves. This is a consequence of original coherence between dates.

Example 5. Lezoux (Auvergne, France). Medieval potter's kiln

In the case of a medieval potter's kiln from Lezoux (Auvergne, France), Maison-de-Retraite-Publique site [Mennessier-Jouannet et al. \(1995\)](#), the Event model dates the last firing of the kiln from baked clay (AM and TL dating) and from charcoals (^{14}C dating). More precisely, dating is based on 3 TL datings (CLER 202a, 202b, 203), 2 AM datings (inclination and declination) and 1 radiocarbon dating (Ly-5212) (Fig. 15). Posterior densities t_i (in color) are very shrunk compared to calibrated densities, especially for archaeomagnetic and TL dates (in black line). Event model gives a HPD interval equal to [575, 864] AD at 95% probability level. Posterior densities for standard deviations σ_i (Fig. 16) are much spread than in the previous example. This comes from the multimodality of AM calibrated dates.

Example 6. Cuers (Provence, France), medieval or modern lime kiln

Last firing date of lime kiln of Cuers (Provence, France), Pas-Redon site ([Vaschalde et al. \(2014\)](#)), has been determined using walls baked clay (AM dating) and charcoals (^{14}C dating). The dating is based on 3 AM datings (inclination, declination and intensity) and on

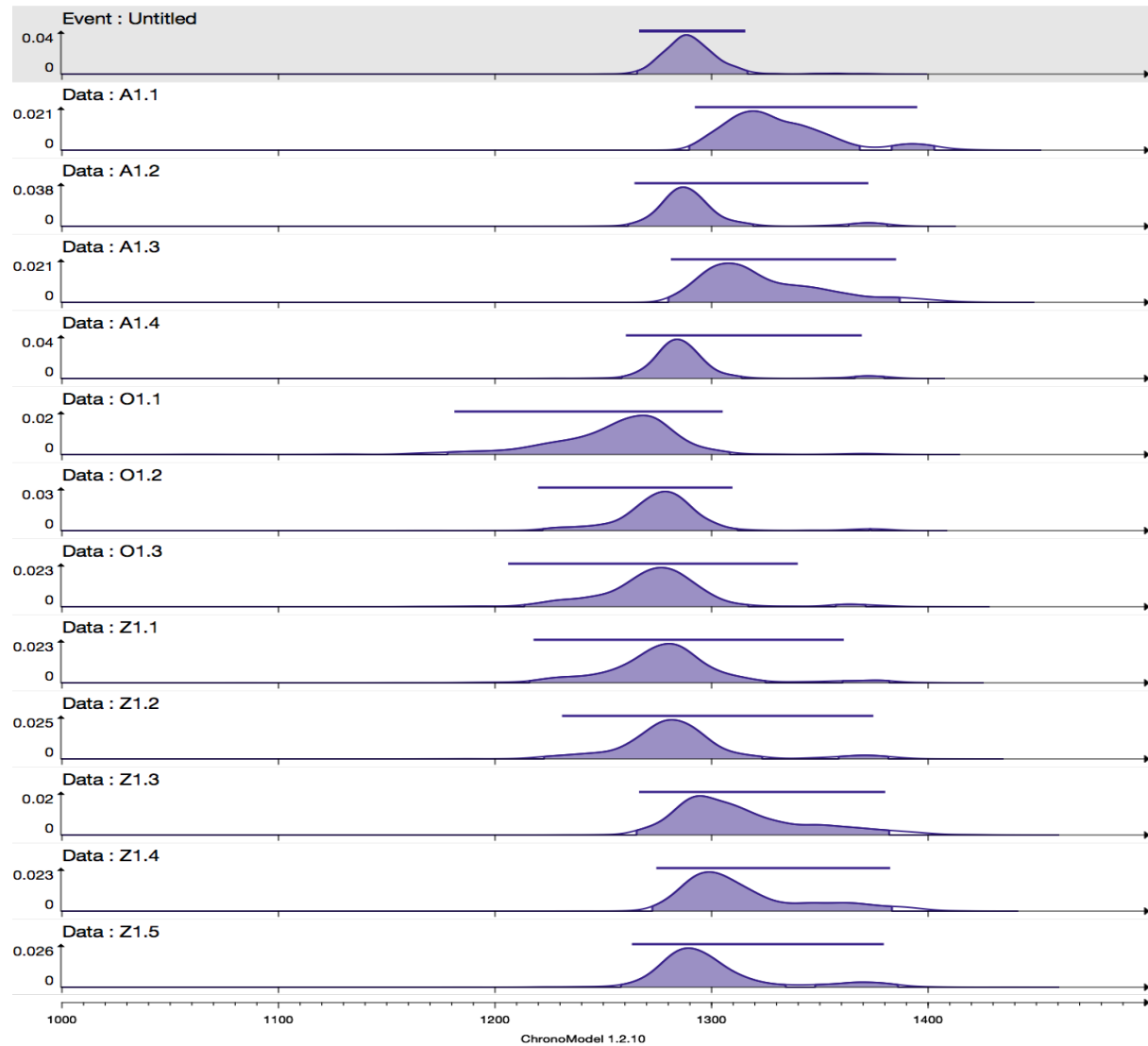


FIGURE 11. Shroud of Turin, Ex. 3. [white background] Posterior densities of t_i and individual posterior calibrated densities (black line) obtained for 12 ^{14}C dates. [gray background] posterior density of the event θ .

2 radiocarbon datings (Poz-42876 and Ly-16086) (Fig. 17). Like in the previous example, posterior densities t_i (in color) are much more shrunk than calibrated densities. Event model gives a double HPD interval [1388, 1548] and [1556, 1616] AD at 95% probability level: we are then in a case of dating indecision. Posterior densities for standard deviations σ_i (Fig. 18) clearly show high values corresponding to AM dating.

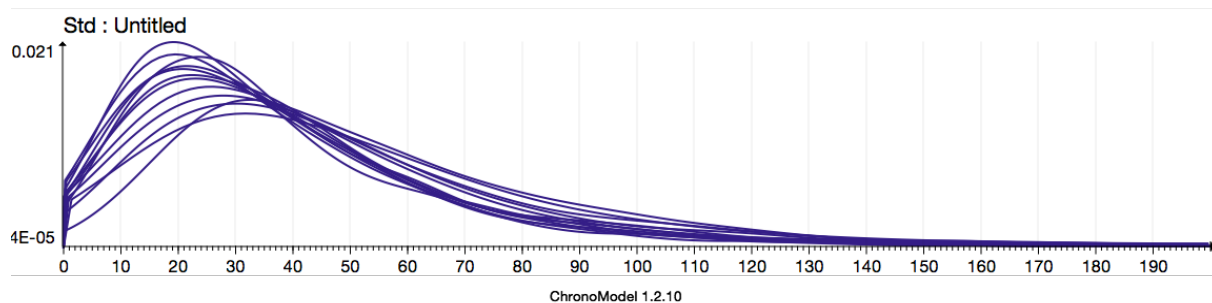


FIGURE 12. Turin, Ex. 3 (Cont.) Posterior densities obtained for standard deviations σ_i .

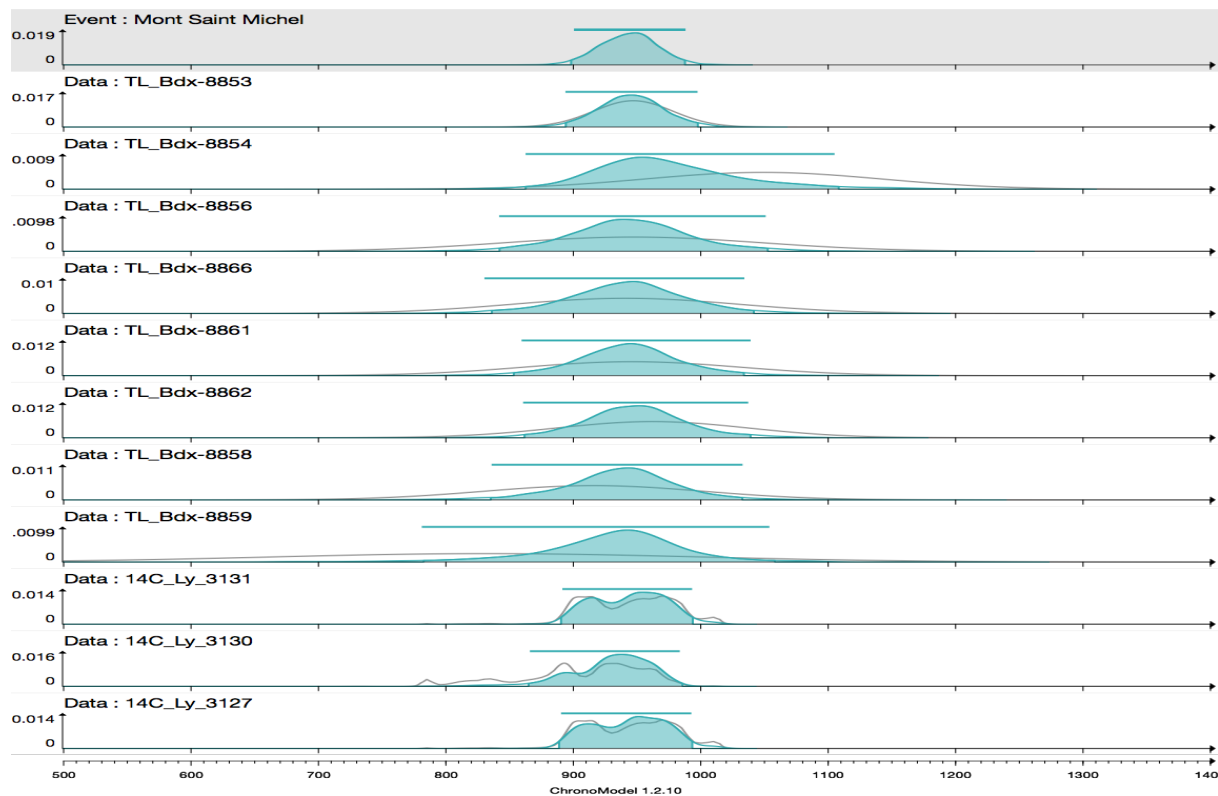


FIGURE 13. Mont-Saint-Michel, Ex. 4. [white background] Posterior densities of t_i and individual posterior calibrated densities (black line) obtained for TL dates and for ^{14}C dates. [gray background] posterior density of the event θ .

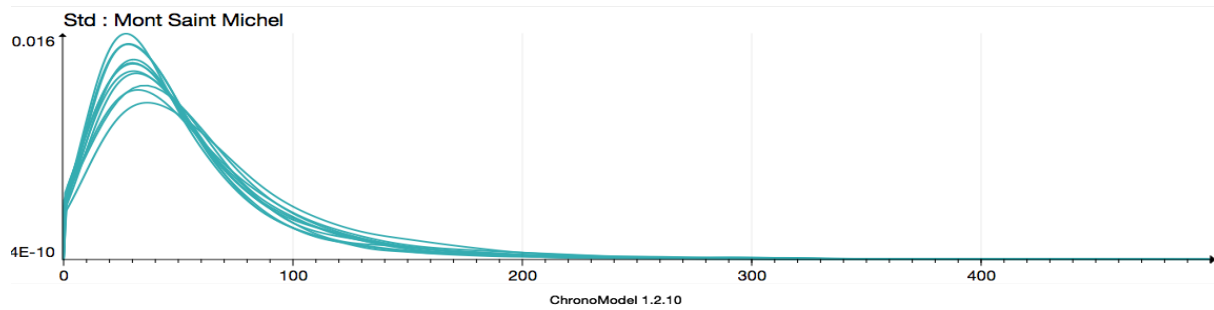


FIGURE 14. Mont-Saint-Michel, Ex. 4 (Cont.). Posterior densities obtained for standard deviations σ_i .

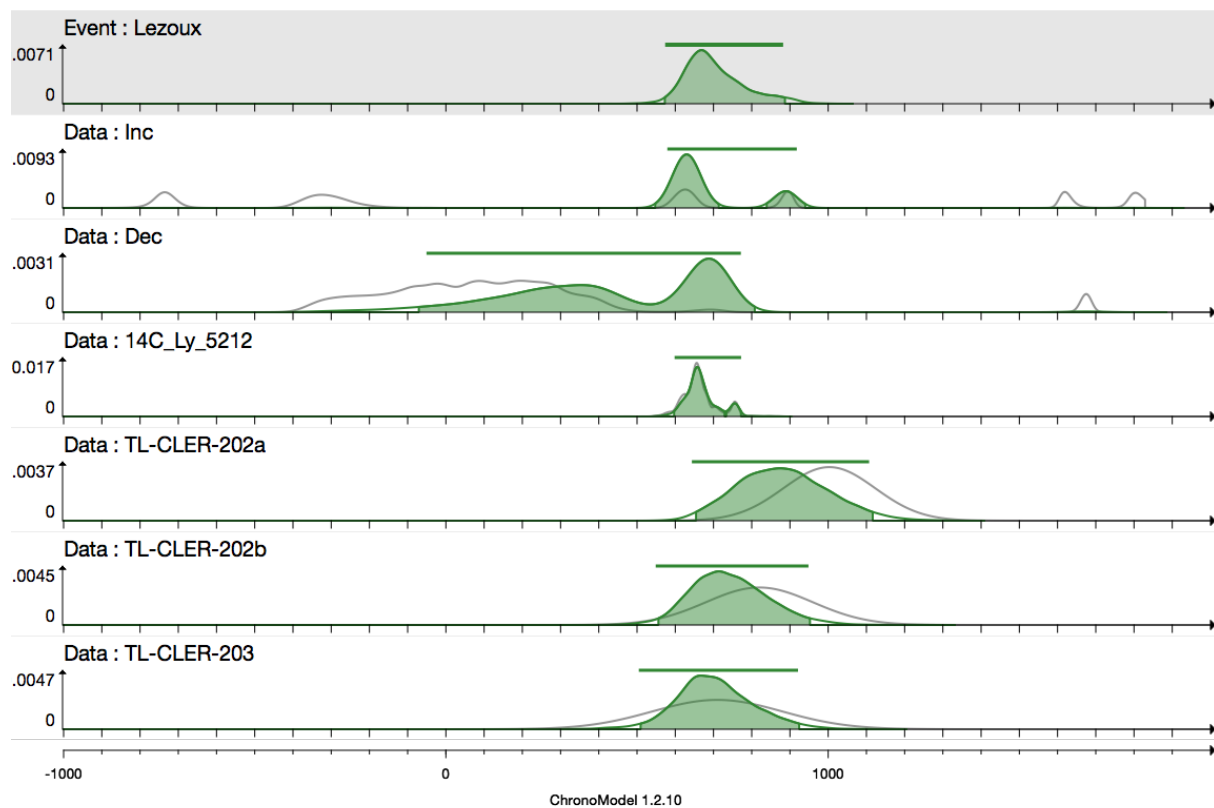


FIGURE 15. Lezoux Ex. 5. [white background] Posterior densities of t_i and individual posterior calibrated densities (black line) obtained for TL dates, for ^{14}C dates and for AM dates. [gray background] Posterior density for Event θ

3.6. **Outliers.** In radiocarbon dating, several Bayesian methods have been proposed to deal with the presence of outliers. The first approach introduced in [Christen \(1994\)](#) incorporates a possible random shift on the measurement M_i . The model with random effect is

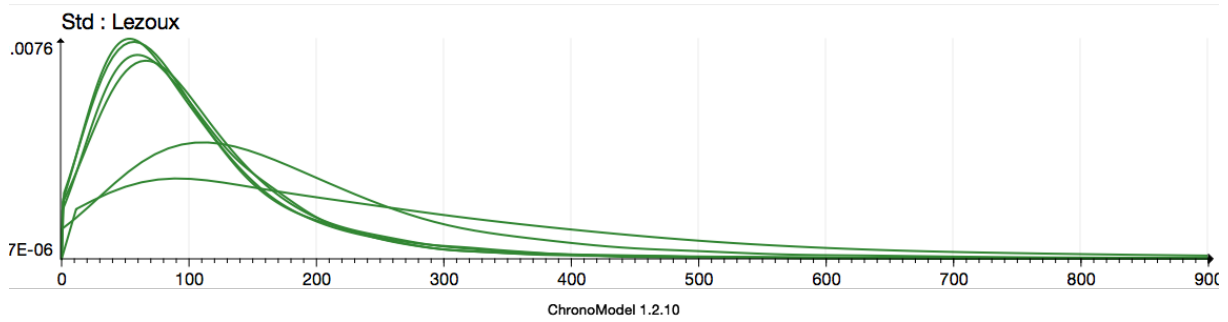


FIGURE 16. Lezoux, Example 5 (Cont.). Posterior densities obtained for standard deviations σ_i .

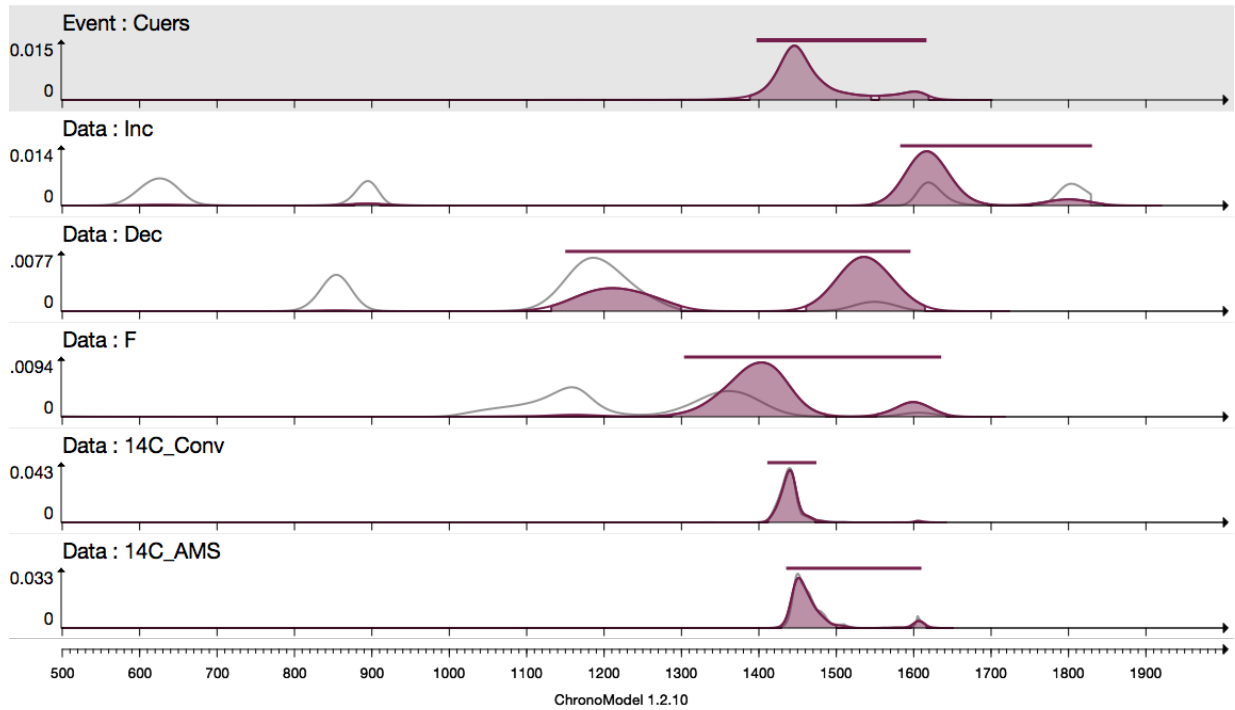


FIGURE 17. Cuers, Ex. 6. [white background] Posterior densities t_i with individual posterior calibrated densities (black). [gray background] posterior density for Event θ .

of the form

$$M_i = g(t) + \Phi_i \delta_i + S_i \epsilon_i \quad (15)$$

where

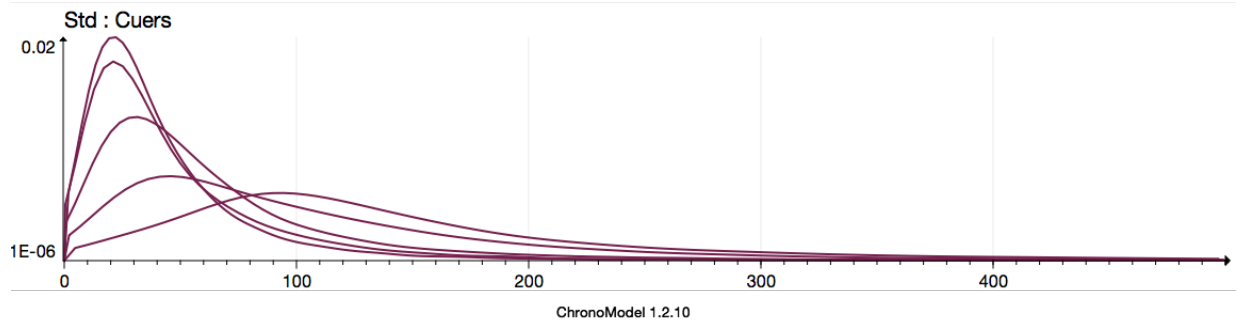


FIGURE 18. Cuers, Ex 6 (Cont.) Posterior densities obtained for standard deviations σ_i .

- the prior for Φ_i is the Bernoulli distribution with parameter p_i . Φ_i takes the value 1 if the measurement requires a shift and 0 otherwise. In practice p_i must be chosen and the recommended value is 0.1 or 0.05.
- δ_i is the lag, the prior for δ_i is the uniform distribution on T .
- ϵ_i is normally distributed with zero mean and variance 1 and $S_i^2 = s_i^2 + \sigma_g^2(t)$.

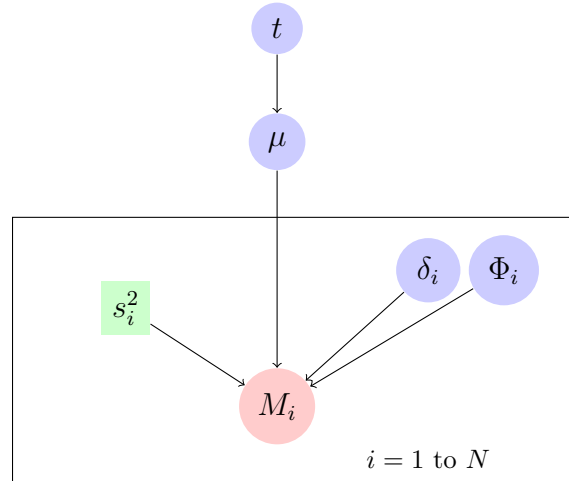


FIGURE 19. DAG of the outlier model given in [Christen \(1994\)](#)

[Bronk Ramsey \(2009b\)](#) proposes different extensions of this model which can be summarized by the following hierarchical Bayesian models :

M1 : s-type outlier model : a shift on the measurement M_i

$$M_i = g(t) + s_i \Phi_i \delta_i 10^u + \epsilon_i \quad (16)$$

Note that r,d-type outlier models are similar.

M2 : Outlier t-type : a shift on the time t :

$$M_i = g(t + \Phi_i \delta_i 10^u) + \epsilon_i \quad (17)$$

where

- Φ_i et ϵ_i are defined as in [Christen \(1994\)](#).
- the distribution of δ_i is a Student's t-distribution with chosen degrees of freedom or a Gaussian distribution.
- u is a scale parameter distributed uniformly on $[0, 4]$

In practice it is difficult to choose between these models because this requires to know if the observation is an outlier in time or an outlier in measurement error.

In the Event model, we assume that the origin of the outlier is unknown, leading ultimately to an offset on the date t_i . Therefore the parameter λ_i in (10) has a role similar to $\Phi_i \delta_i$ in the t-type outlier model (M2).

The variance σ_i^2 indicates if the observation is an outlier. Indeed if one measurement M_i gives an off-trend calibrated date t_i compared to other calibrated dating, the posterior distribution of σ_i will have a large mean, and thus inducing an automatic penalization of the date t_i contributing to the event.

Example 7. Synthetic data with outlier

In order to illustrate these properties, we consider a synthetic Event example composed of four measurements Gaussian distributed around 800, 850, 900 and 1500 with standard deviation 30, and calibrated using the simple linear transformation $M = g(t) = t$. This example (Fig. 20) shows that an outlying date (here 1500) has always no influence onto Event result. The HPD interval obtained with the four data is [795, 914] AD at 95% while HPD obtained with the three well grouped data is [791, 909] at 95%. Three of the posterior distributions of the standard deviations σ_i ($i=1, \dots, 3$) remain near zero while the standard deviation of data 1500 is high because of its outlying position. This behaviour already observed in the first examples (see posterior standard deviation densities in figures 3, 5, 12, 14, 16 and 18 demonstrates that Event model appears to be a robust statistics for calculating posterior mean of the date θ with very weak assumption on prior densities.

Example 8. Tell Qasile, context X

Here robustness and ease of implementation is tested on eleven radiocarbon dates determined for context X of Tell Qasile and modelled in ([Bronk Ramsey, 2009b](#), table 2, p. 1028 and 1029). Oxcal calculation used R-combine function with s-type outlier detection option and provided two HPD intervals equal to $[-1054; -970]$ and $[-962; -934]$ at 95%. Event model (Fig. 21a) gives a mono-modal posterior density and a single HPD interval

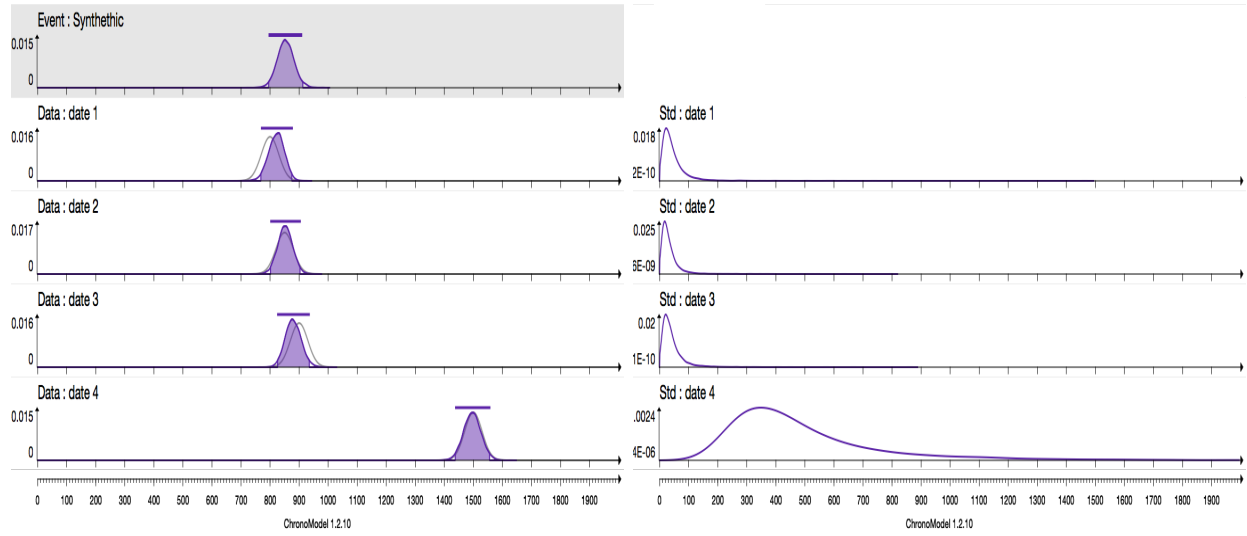


FIGURE 20. Synthetic data, Ex 7. [left] Posterior densities t_i (white background) and posterior density for Event θ (gray background). The individual posterior calibrated densities are superimposed in black. [right] Posterior densities of the standard deviations σ_i .

equal to $[-1050; -951]$ at 95% which is very similar to the two merged Oxcal intervals. Posterior densities for standard deviations σ_i are very similar (Fig. 21) except for samples QS1 and QS6 which show higher posterior values and thus appears as outliers (these were also detected by Oxcal treatment).

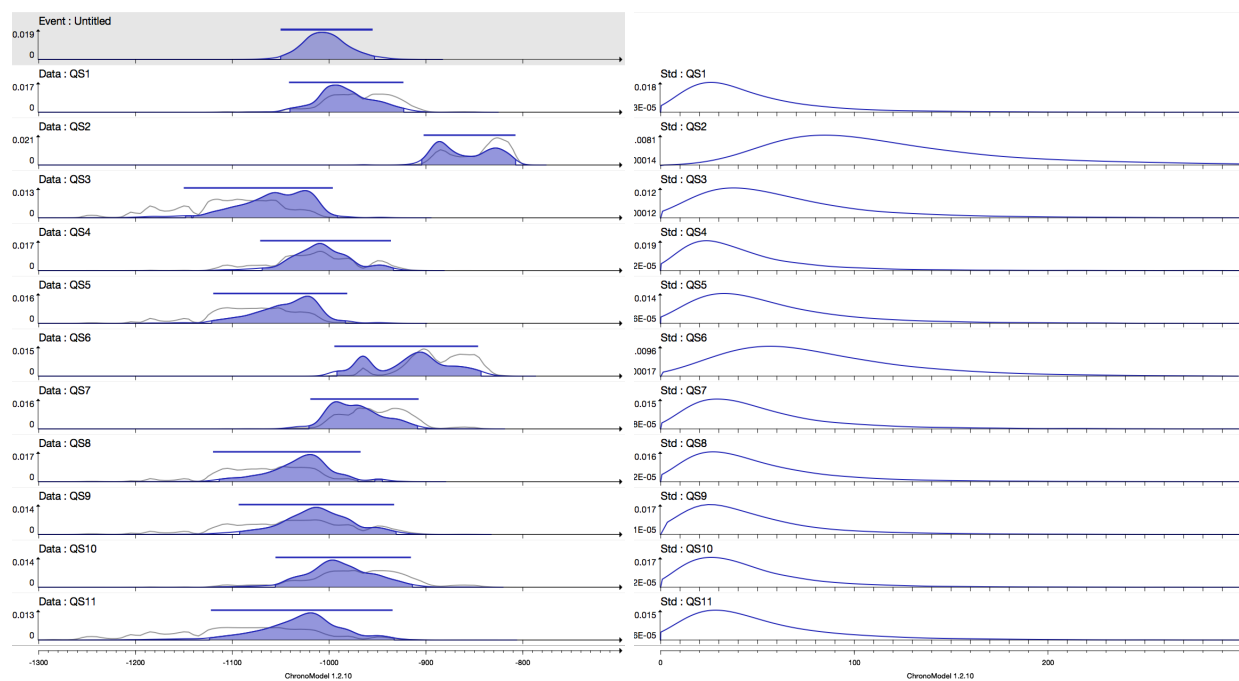


FIGURE 21. Tell Qasile, Ex. 8. [left] Posterior densities t_i for ^{14}C dates and posterior density for Event θ (gray background). . The individual posterior calibrated densities are superimposed in black. [right] Posterior densities obtained for standard deviations σ_i .

3.7. Calibrated Event for wiggle-matching. The "wiggle-matching" model combines radiocarbon dating and dendrochronology. The ^{14}C datings are carried out on tree-ring samples separated by a known number of tree-rings (see Manning et al., 2010; Galimberti and Ramsey, 2004; Christen and Litton, 1995, for instance).

In this case, the calibrated dates t_i should be shifted in order to be contemporaneous to the event date θ . So we adapt our event model to wiggle-matching as follows. We consider that the event date θ corresponds to the date of a chosen reference tree-ring (for instance the oldest tree-ring, see Example 9).

We denote by δ_i the number of years corresponding to this lag in time. We convert the number of estimated tree-rings into years, assuming that one tree-ring is equal to one year. By convention, δ_i is positive (resp. negative) when t_i is older (resp. younger) than θ .

We rewrite equation (10) as follows

$$t_i = \theta - \delta_i + \sigma_i \lambda_i \quad (18)$$

Moreover it is easy to take into account some cases with unknown δ_i . It is necessary to build a prior distribution for $(\delta_1, \dots, \delta_n)$. The information available on the parameter δ_i is often expressed of the form $\delta_i \in]\delta_{\min}, \delta_{\max}[$. So the prior distribution can be chosen uniform on this interval. To relax the constraint on the support we can also choose a Gaussian prior with mean $\frac{1}{2}(\delta_{\min} + \delta_{\max})$ and variance $\frac{1}{12}(\delta_{\max} - \delta_{\min})^2$.

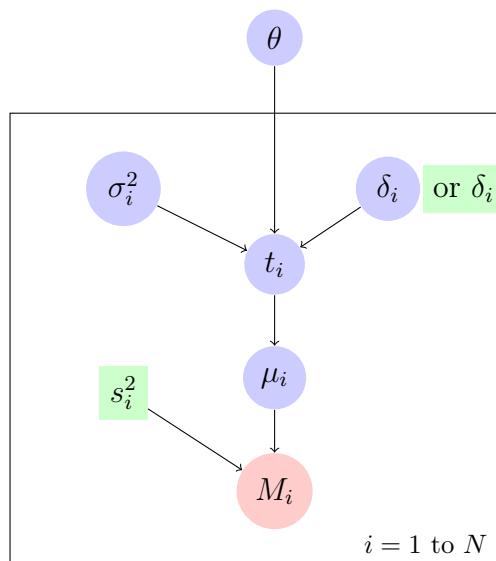


FIGURE 22. DAG for the wiggle matching model. The shifts δ_i can be known or estimated

Example 9. Gordion juniper dendrochronology (Central Anatolia)

An application of the Event wiggle-matching model is presented here in the case of the Gordion juniper dendrochronology (See [Manning and Kromer, 2011](#), table 1). 35 samples of this sequence, from relative tree-rings centered at 776.5-1025.5 have been dated in the Heidelberg radiocarbon Laboratory. The samples are calibrated with IntCal04.14c curve ([Reimer et al. \(2004\)](#)) and are separated with known gaps taking values between 1 and 19 years over a range of 249 years. δ_i is the gap between dated tree-ring and reference. According to [Manning and Kromer \(2011\)](#), we fix the oldest tree-ring as reference (it means that $\delta_1 = 0$). The Event model gives a HPD interval equal to [-1744, -1719] at 95% probability level. In comparison, the model implemented in Oxcal, by using D-Sequence and Gap functions with Outlier-Model("SSimple",N(0,2),0,"s"), gives a HDP interval equal to [-1734, -1724] at 95%.

The event model provides an estimation less accurate than the model considered in [Manning and Kromer \(2011\)](#). The difference on the length of the HPD region is due to the event structure which increases the variance of the posterior distribution. However our approach brings robustness. As an illustration, we modify artificially the dataset by adding outliers :

Figure 23 gives the estimation obtained by the event model for both samples :

- the original Gordion dataset analyzed in [Manning and Kromer \(2011\)](#),
- the same dataset contaminated with 11 outliers. We modify the 14C ages as described in the table below. We keep the same experimental variances on the 14C ages.

sample number with Manning and Kromer (2011) notations	modified 14C age (BP)
20144, 27605	3100
20137, 25792,20155	3600
20157,20141,20147,25793,20153,27612	3700

Figure 23 shows that the posterior distribution of the event date is not sensitive to the presence of these outliers.

On original dataset, the HPD interval for θ is equal to [-1744, -1719] at 95%. This result is very close to the one obtained with Oxcal (v.4.1) using sequence model with s-type outlier detection : [-1734,-1724] at 95%.

On the contaminated sample, the model considered in [Manning and Kromer \(2011\)](#) cannot be estimated with Oxcal software. It does not return estimations because of poor

agreement indices. The event model gives an HPD interval for θ equal to $[-1749, -1717]$ at 95%.

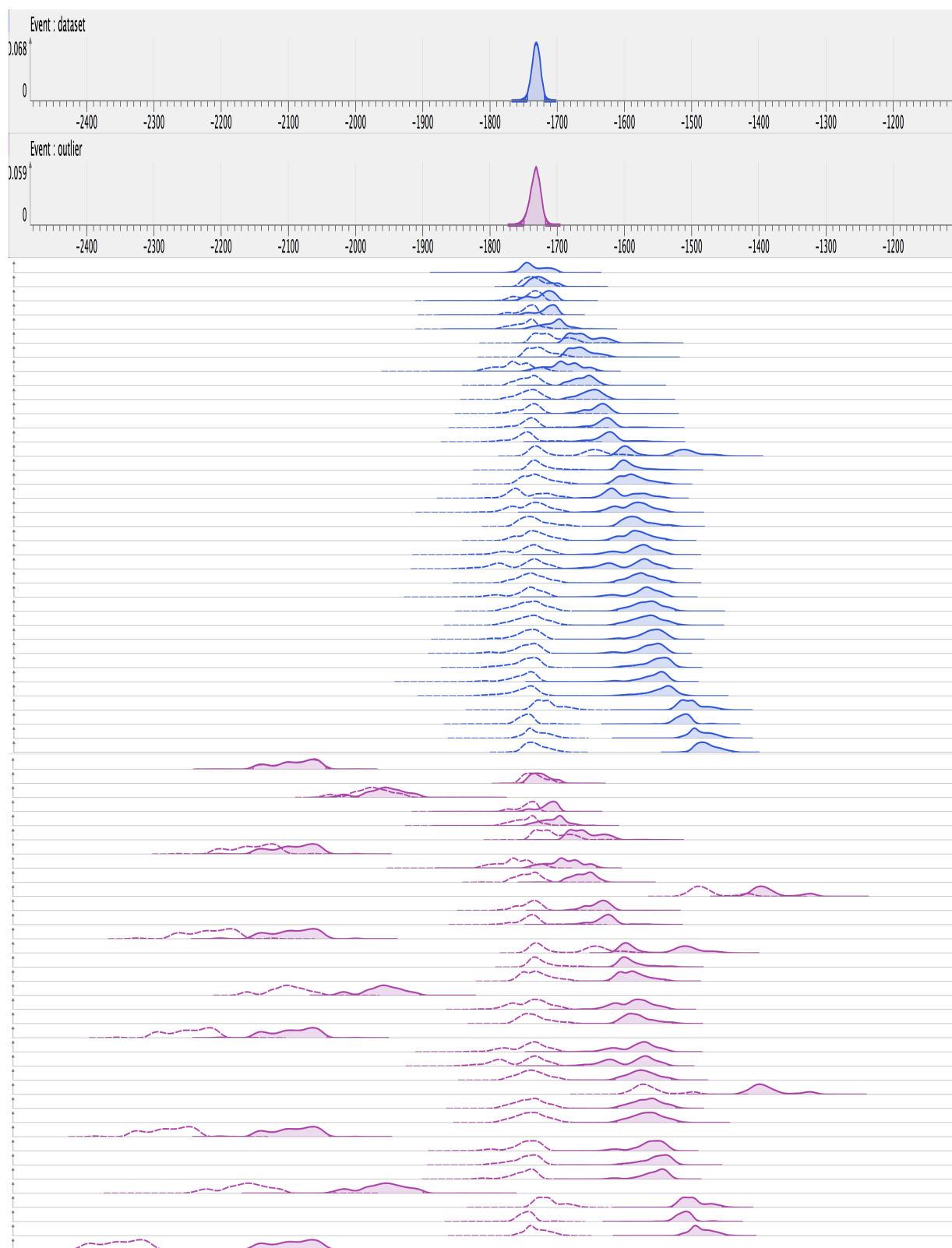


FIGURE 23. Gordion juniper dendrochronology (Central Anatolia). Posterior densities of the dates t_i (white background) and the Event date θ (gray background) obtained on original Gordion dataset (blue) and on a contaminated version with 11 outliers (red)

4. CONCLUSION

The Bayesian model we propose to combine measurements or dates in order to get respectively a mean of measurements or the date of an event is very simple. It allows to automatically penalise outliers. In chronological problems, the Event model assumes that the dated artefacts are contemporaneous and consequently dates can be combined whatever the dating method is (chronometric methods, typo-chronology, history). Moreover, in the Chronomodel software, the event model appears as the first fundamental stone on which stratigraphic constraints and phasing can be put on inside much more complicated chronological models.

5. APPENDIX

5.1. **Construction of ML estimate given by (2).** The likelihood function of the model is

$$L = \prod_{i=1}^n p(M_i|\mu, s_i^2) = \prod_{i=1}^n \frac{1}{s_i\sqrt{2\pi}} e^{\frac{-1}{2s_i^2}(M_i-\mu)^2}.$$

The derivative of this function with respect to μ is equal to zero when

$$\mu = \sum_{i=1}^n \frac{1}{s_i^2} M_i \left(\sum_{i=1}^n \frac{1}{s_i^2} \right)^{-1}$$

This is a maximum, and so the MLE estimate is

$$\hat{\mu}_n = \frac{\sum_{i=1}^n \frac{M_i}{s_i^2}}{\sum_{i=1}^n \frac{1}{s_i^2}}$$

(see [Ward and Wilson \(1978\)](#)).

5.2. **Estimation of μ with random effect.** The likelihood function is given by

$$L_H = \prod_{i=1}^n p(M_i|\mu_i)p(\mu_i|\mu, \sigma^2) \tag{19}$$

where

$$p(M_i|\mu_i) = \frac{1}{s_i\sqrt{2\pi}} e^{\frac{-1}{2s_i^2}(M_i-\mu_i)^2}$$

and

$$p(\mu_i|\mu, \sigma^2) = \frac{1}{\sigma\sqrt{2\pi}} e^{\frac{-1}{2\sigma^2}(\mu_i-\mu)^2}$$

We integrate with respect to the hyper parameters μ_i ($i=1, \dots, n$) to obtain the conditional density :

$$p(M_i|\mu, \sigma^2) = \frac{1}{\sqrt{2\pi(s_i^2 + \sigma^2)}} \exp \left\{ \frac{-1}{2(s_i^2 + \sigma^2)} (M_i - \mu)^2 \right\} \quad (20)$$

According to the independence of M_i , $i = 1, \dots, n$, the likelihood function is

$$L = \prod_{i=1}^n \sqrt{\frac{W_i}{2\pi}} \exp \left\{ \frac{-1}{2} \sum_{i=1}^n W_i (M_i - \mu)^2 \right\} \quad (21)$$

where

$$W_i = \frac{1}{s_i^2 + \sigma^2} \quad (22)$$

By canceling the partial derivatives of $\ln(L)$ with respect to σ and μ we get the following system of equations

$$\begin{cases} \mu = \frac{1}{W} \sum_{i=1}^n W_i M_i \\ \sum_{i=1}^n W_i - \sum_{i=1}^n W_i^2 (M_i - \mu)^2 = 0 \end{cases} \quad (23)$$

where $W = \sum_{i=1}^n W_i$. This system leads to an equation in σ^2 , which does not admit an explicit solution. if there is a strictly positive solution denoted $\hat{\sigma}_n^2$, then we can use a numerical method, e.g. bisection Method, to approximate the solution.

By substituting in the equation (23-1), we estimate the parameter μ by

$$\tilde{\mu}_n = \sum_{i=1}^n \frac{M_i}{s_i^2 + \hat{\sigma}_n^2} \left(\sum_{i=1}^n \frac{1}{s_i^2 + \hat{\sigma}_n^2} \right)^{-1} .$$

The existence problem is illustrated in the particular case $s_i^2 = s^2$ for $i = 1, \dots, n$. In this case we get an explicit solution for the system (23). The estimate of μ is the empirical mean

$$\tilde{\mu}_n = \frac{1}{n} \sum_{i=1}^n M_i = \bar{M}_n$$

and the variance σ^2 is estimated by

$$\hat{\sigma}_n^2 = \begin{cases} \frac{1}{n} \sum_{i=1}^n (M_i - \tilde{\mu}_n)^2 - s^2 & \text{if } s^2 < \frac{1}{n} \sum_{i=1}^n (M_i - \tilde{\mu}_n)^2 \\ 0 & \text{otherwise} \end{cases}$$

If $s^2 = 0$ then the estimate of σ^2 is the empirical variance :

$$\hat{\sigma}_n^2 = \frac{1}{n} \sum_{i=1}^n (M_i - \bar{M}_n)^2$$

This situation corresponds to strong assumptions on the variances. Indeed the experimental variance on the measurements s_i^2 are nul and the individual variances σ_i^2 are set equal to σ^2 . Therefore it is a very restrictive choice which does not reflect errors carried by measurements or dating.

5.3. Nonexistence of the Maximum Likelihood Estimate when $\sigma_i^2 \neq 0$. According to the independence of M_i , $i = 1, \dots, n$, the likelihood function is

$$L(\mu, \sigma_1, \dots, \sigma_n) = \prod_{i=1}^n \sqrt{\frac{W_i}{2\pi}} \exp \left\{ \frac{-1}{2} \sum_{i=1}^n W_i (M_i - \mu)^2 \right\} \quad (24)$$

where

$$W_i = \frac{1}{s_i^2 + \sigma_i^2}.$$

If the ML estimate of μ exists, then the variances σ_i^2 are solution of the following system

$$\begin{cases} \mu = \sum_{i=1}^n \frac{1}{s_i^2 + \sigma_i^2} M_i \left(\sum_{i=1}^n \frac{1}{s_i^2 + \sigma_i^2} \right)^{-1} \\ \sigma_i^2 = (M_i - \mu)^2 - s_i^2 \end{cases} \quad \text{pour tout } i = 1, \dots, n \quad (25)$$

By substituting the expression of σ_i^2 in (24), we get :

$$\tilde{L}(\mu) = \sum_{i=1}^n \frac{1}{|M_i - \mu|}$$

M_1, \dots, M_n are the singular points of the function \tilde{L} (in the sense that $\lim_{\mu \rightarrow M_i} \tilde{L}(\mu) = +\infty$ for all i). Therefore the ML estimate is not defined. This difficulty can be overcome using the Bayesian approach.

REFERENCES

- Bronk Ramsey, C. (2009a). Bayesian analysis of radiocarbon dates. *Radiocarbon*, 51(1):337–360.
- Bronk Ramsey, C. (2009b). Dealing with outliers and offsets in radiocarbon dating. *Radiocarbon*, 51(3):1023–1045.
- Buck, C. (2004). Bayesian chronological data interpretation: Where now? In Buck, C. and Millard, A., editors, *Tools for Constructing Chronologies*, volume 177 of *Lecture Notes in Statistics*, pages 1–24. Springer London.
- Buck, C. E., Litton, C. D., and G., C. W. (1996). *The Bayesian Approach to Interpreting Archaeological Data*. Chichester, J.Wiley and Son, England.

- Christen, J. and Litton, C. (1995). A bayesian approach to wiggle-matching. *Journal of Archaeological Science*, 22(6):719 – 725.
- Christen, J. A. (1994). Summarizing a set of radiocarbon determinations: a robust approach. *Applied Statistics*, 43(3):489–503.
- Chronomodel Software (2015). Chronological modelling of archaeological data using bayesian statistics. www.chromodel.fr, v1.1.
- Congdon, P. D. (2010). *Applied Bayesian hierarchical methods*. CRC Press, Boca Raton, FL.
- Damon, P. E. (1989). Radiocarbon dating of the shroud of turin. *Nature*, 337(6208):611–615.
- Daniels, M. J. (1999). A prior for the variance in hierarchical models. *Canad. J. Statist.*, 27(3):567–578.
- Galbraith, R. F. and Green, P. (1990). Estimating the component ages in a finite mixture. *Radiation Measurements*, 17:197–206.
- Galbraith, R. F., Roberts, R. G., Laslett, G. M., Yoshida, H., and Olley, J. M. (1999). Optical dating of single and multiple grains of quartz from jinmium rock shelter, northern australia: part i, experimental design and statistical models*. *Archaeometry*, 41(2):339–364.
- Galimberti, M. and Ramsey, C. B. (2004). Wiggle-match dating of tree-ring sequences. *Radiocarbon*, 46(2):917–924.
- Litton, C. D. and Buck, C. E. (1995). The bayesian approach to the interpretation of archaeological data. *Archaeometry*, 37(1).
- Manning, S., Kromer, B., Ramsey, C. B., Pearson, C., Talamo, S., Trano, N., and Watkins, J. (2010). 14c record and wiggle-match placement for the anatolian (gordion area) juniper tree-ring chronology 1729 to 751 cal bc, and typical aegean/anatolian (growing season related) regional 14c offset assessment. *Radiocarbon*, 52(4).
- Manning, S. W. and Kromer, B. (2011). Radiocarbon dating archaeological samples in the eastern mediterranean, 1730 to 1480 bc: further exploring the atmospheric radiocarbon calibration record and the archaeological implications*. *Archaeometry*, 53(2):413–439.
- Mennessier-Jouannet, C., Bucur, I., Evin, J., Lanos, P., and Miallier, D. (1995). Convergence de la typologie de céramiques et de trois méthodes chronométriques pour la datation d’un four de potier à lezoux (puy-de-d’ôme). *Revue d’Archéométrie*, 19:37–47.
- Ramsey, C. B. and Lee, S. (2013). Recent and planned developments of the program oxcal. *Radiocarbon*, 55.
- Reimer, P. J., Baillie, M. G. L., Bard, E., Bayliss, A., Beck, J. W., Bertrand, C. J. H., Blackwell, P. G., Buck, C. E., Burr, G. S., Cutler, K. B., Damon, P. E., Edwards,

- R. L., Fairbanks, R. G., Friedrich, M., Guilderson, T. P., Hogg, A. G., Hughen, K. A., Kromer, B., McCormac, G., Manning, S., Bronk Ramsey, C., Reimer, R. W., Remmele, S., Southon, J. R., Stuiver, M., Talamo, S., Taylor, F. W., van der Plicht, J., and Weyhenmeyer, C. E. (2004). Intcal04 terrestrial radiocarbon age calibration, 0-26 cal kyr bp. *Radiocarbon*, 46(3):1029–1058.
- Sapin, C., Bayle, M., Buttner, S., Guibert, P., Blain, S., Lanos, P., Chauvin, A., Dufresne, P., and Oberlin, C. (2008). Archeologie du bati et archeometrie au mont-saint-michel, nouvelles approches de notre-dame-sous-terre. *Archeologie medievale*, 38:71–122.
- Sitzia, L., Bertran, P., Boulogne, S., Brenet, M., Crassard, R., Delagnes, A., Frouin, M., Hatte, C., Jaubert, J., Khalidi, L., Messenger, E., Mercier, N., Meunier, A., Peigne, S., Queffelec, A., Tribolo, C., and Macchiarelli, R. (2012). The paleoenvironment and lithic taphonomy of shi bat dihya 1, a middle paleolithic site in wadi surdud, yemen. *Geoarchaeology*, 27:471–491.
- Spiegelhalter, D. J., Abrams, K. R., and Myles, J. P. (2004). *Bayesian Approaches to Clinical Trials and Health-Care Evaluation*. Wiley, Chichester.
- Vaschalde, C., Hervé, G., Lanos, P., and Thiriot, J. (2014). La datation des structures de cuisson: intégration de l’archéomagnétisme et du radiocarbone, apports de l’anthracologie. *Archéologie Médiévale*, 44:1–16.
- Vibet, M.-A., Philippe, A., Lanos, P., and Dufresne, P. (2015). Chronomodel user’s manual. www.chromodel.fr.
- Ward, G. K. and Wilson, S. R. (1978). Procedures for comparing and combining radiocarbon age determinations: a critique. *Archaeometry*, 20(1):19–31.